Available online at www.sciencedirect.com

ScienceDirect

Acta Materialia 67 (2014) 335–341

Acta MATERIALIA

www.elsevier.com/locate/actamat

Diffusional constrained crystal nucleation during peritectic phase transitions

S. Griesser [a,*], M. Reid [a], C. Bernhard [b], R. Dippenaar [a]

[a] Faculty of Engineering and Information Sciences, University of Wollongong, Wollongong, Australia
[b] University of Leoben, Leoben, Austria

Received 4 November 2013; accepted 11 December 2013

Abstract

The casting behaviour, microstructure formation and resulting mechanical properties of materials that undergo a peritectic phase transition during solidification are largely determined by the kinetics of this high-temperature phase transformation during the production process. However, current nucleation models do not accurately predict the nucleation behaviour and phase transition kinetics in many polycrystalline materials. Utilizing a newly developed experimental technique, we have performed in situ observations to study the nucleation behaviour of a newly forming intermediate phase by using the peritectic phase transition in Fe–C and Fe–Ni alloys as examples. In our experiments as well as by using thermodynamic and kinetic arguments we demonstrate that nucleation of a new intermediate (peritectic) phase can be constrained in the presence of solute diffusion fields that form during primary solidification due to an increase in the Gibbs free energy barrier for nucleation. We found a strong correlation between the magnitude of these diffusion fields and the resulting nucleation undercooling required for the formation of a new phase. Our study casts new light on, and clarifies for the first time, the much-debated underpinning reason for the occurrence of massive phase transformations occurring during solidification processing at large nucleation undercoolings. These new insights contribute to the improvement of nucleation theory and allow more accurate predictions on nucleation events and, in turn, physical properties of materials that undergo phase transitions in the course of materials production processes.

Keywords: Nucleation; Peritectic solidification; Massive transformation; Gibbs energy

1. Introduction

The formation of crystalline solids from solution is fundamental to many natural and industrial processes. The crystallization process begins with nucleation, which plays a central role in determining the structure and size distribution of the crystals [1]. These crystallization processes are important in a variety of fields such as medical engineering, nanoparticle production, protein crystallization, and the solidification of metals and alloys. Hence, it is critically important to understand the fundamental scientific principles underpinning this initial, often limiting, step in the phase transformation process. Only with such understanding can we exercise control over and optimize solidification structures of significance to our industries that work towards the enhancement of the quality of human life.

In the classical picture, nucleation is a stochastic process in which compositional fluctuations induce the formation of clusters that are unstable with respect to dissolution. Clusters increase in both size and free energy due to the creation of an interface until a threshold is crossed, whereupon the free energy reduction due to forming the new phase overcomes the penalty for creating an interface, and growth proceeds spontaneously. However, recent observations have clearly suggested that this classical theory of nucleation often fails to predict nucleation

* Corresponding author.
E-mail address: sg045@uowmail.edu.au (S. Griesser).

1359-6454/$36.00
http://dx.doi.org/10.1016/j.actamat.2013.12.018

behaviour during phase transitions [2,3], such as the peritectic phase transition. Materials that undergo the peritectic phase transition include technologically important materials such as steel, copper and aluminium alloys, nickel-based superalloys and titanium aluminides as well as magnetic and electronic materials for the superconductor industry [4–6]. For instance, the production of large single-crystal (RE)–Ba–Cu–O superconductors is based on the formation of the RE-123 phase through a peritectic reaction [7] at high undercoolings in order to improve the kinetics of the reaction [8]. The pivotal role nucleation can play in peritectic systems can be illustrated with reference to the Al–Ti system. The primary intermetallic Al_3Ti phase that forms in the course of the peritectic transition can act as a nucleant for aluminium grains [9–12] and these nucleation events are fruitfully utilized to achieve grain refinement during casting or welding.

The peritectic phase transition occurring in the Fe–C system at 1768 K is arguably the most important peritectic from an industrial point of view since much of the more than 1.5 billion tonnes of steel produced annually undergoes this phase transition. Moreover, this peritectic reaction and subsequent peritectic transformations have been implicated in a myriad of difficulties encountered in the production process that hamper production rates and result in inferior product quality [13]. In the Fe–C system, the liquid and primary solid δ-ferrite phases produce a second γ-austenite solid phase ($\delta + L \rightarrow \gamma$) with a different crystal structure than δ. Under equilibrium conditions, nucleation of γ occurs at δ grain boundaries that are in contact with liquid at a temperature just below the equilibrium peritectic temperature, T_P^E. Following the nucleation event, the γ-phase grows along the liquid/δ interface (termed the peritectic reaction) and subsequently further into the δ and into the remaining liquid (the peritectic transformations). However, at high cooling rates the δ to γ phase transition is suppressed and a transformation occurs by a massive-type of phase transformation [14–16]. The mechanism by which this massive-type of transition occurs has never been satisfactorily explained notwithstanding the fact that it is this phase transition that seems to be the root cause of the quality defects encountered in the continuous casting of steel [16]. Jacot et al. [17] recently showed that solute-trapping-free massive transformation can occur above the limit of absolute stability, i.e. at high velocities of the transformation front without the need of high nucleation undercoolings. However, linked to the occurrence of the massive-type of transformation in peritectic systems is the observation that significant undercooling is required to induce this massive-type of transformation, which in turn suggests a mechanism linked to a nucleation constraint. The occurrence of high nucleation undercooling in peritectic systems and the resulting massive transformation of δ to γ has frequently been reported [14–15,18–20], but a satisfactory explanation for these nucleation constraints is still lacking. The application of classical nucleation theory (CNT) [21] to explain the high nucleation undercooling in peritectic systems has had limited success since the experimentally determined temperature at which γ nucleation occurs (undercooling below the equilibrium peritectic temperature) is much lower than can be explained by this theory [18,19]. Fundamental understanding of the nucleation process in peritectic systems is still in its infancy and the present study is aimed at providing new insights with respect to constrained nucleation events.

2. Experimental

Progress in the study of nucleation behaviour in metallic systems during peritectic solidification has been inhibited by the difficulties encountered in conducting experiments at the elevated temperatures at which they occur. However, the development of techniques for the in situ study of high-temperature phase transformations, such as transmission X-ray observation, the Bridgman furnace and high-temperature laser-scanning confocal microscopy provides the ability to capture solidification processes in real time and high resolution as well as to observe and measure the morphology and kinetics of phase transformations. We employed a concentric solidification technique [22–25] within a high-temperature laser-scanning confocal microscope to study in situ the nucleation behaviour and transformation kinetics of the peritectic phase transition in Fe–C and Fe–Ni alloys as examples of the nucleation behaviour of a newly forming intermediate phase. Specimens (9.8 mm diameter and 250 μm thick) are placed beneath a quartz viewpoint in a gold-plated, ellipsoidal infrared heating furnace under an ultrahigh-purity argon atmosphere. A 1.5 kW halogen lamp located at one focal point of the ellipsoidal cavity heats the specimen positioned at the other focal point. Capitalizing on a radial thermal gradient across the specimen, a

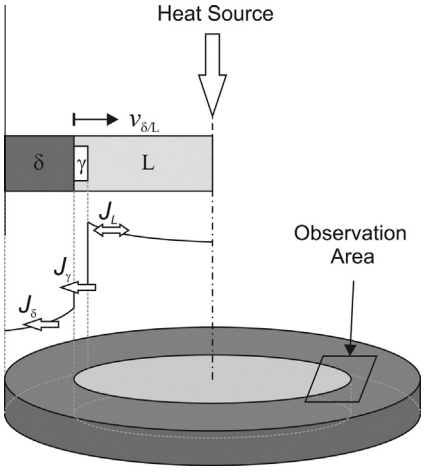

Fig. 1. Schematic illustration of the concentric solidification technique for HTLSCM. The sketch on the left hand side shows the concentration distribution and solute diffusion fluxes J_i in the vicinity of a γ cluster at the δ/*L* interface.

centralized pool of liquid is formed, which is surrounded by a solid rim of the same material [22], as illustrated in Fig. 1.

In Fig. 2 the initial conditions prior to solidification are illustrated with respect to the Fe–C phase diagram. Specimens are heated to an initial temperature T_i within the two-phase region $\delta + L$, held isothermally at this temperature for homogenization and subsequently solidified at a previously determined cooling rate. The resulting propagation of the L/δ interface is tracked using specially developed image-processing software [26] until nucleation and growth of γ occurs at this interface. A benefit of the concentric geometry of the experimental arrangement is that the phase fractions can be measured in situ at any given moment during the experiment, enabling an accurate determination of the fraction of primary solidified δ, $\Delta f_S(\delta) = f_S(T_P) - f_S(T_i)$, prior to γ nucleation.

3. Results

When a specimen of Fe–C alloy is solidified from an initial temperature just above T_P^E ($T_i = 1769$ K) at a cooling rate of 1 K min^{-1}, nucleation of γ occurs at $T_P = 1768$ K (i.e. T_P^E), very close to chemical and thermal equilibrium, as predicted by CNT. Once nucleation of γ occurs, immediate subsequent growth of γ (i.e. peritectic reaction) continues at an equal rate along the L/δ interface in both directions from the nucleation site as shown in Fig. 3.

By contrast, on cooling at the same rate but from higher initial temperatures ($T_i > 1769$ K), nucleation of γ occurs at temperatures well below T_P^E (i.e. at higher nucleation undercooling, ΔT_P). This observation cannot be explained by CNT. Further analysis on this phenomenon revealed that the higher fraction of primary solidified δ, $\Delta f_S(\delta)$, that accompanies the higher initial temperature (as observable in the corresponding phase diagram, see Fig. 2) leads to the creation of pronounced solute concentration gradients

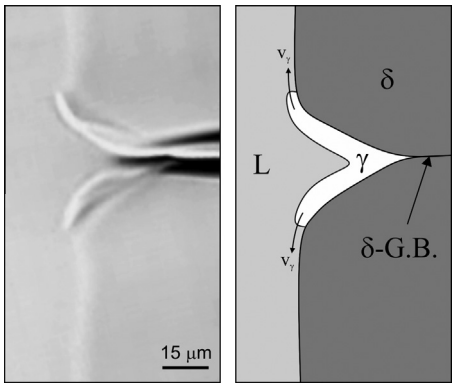

Fig. 3. Nucleation and growth of γ at a δ-grain-boundary in contact with L in a Fe–0.43 wt.%.

in δ due to partitioning and insufficient back-diffusion. These concentration gradients result in the diffusion of solute (i.e. carbon) from the liquid, through the L/δ interface (γ nucleation site) into δ and the higher the magnitude of this flux, the higher the undercooling before γ nucleation initiates. An increase in $\Delta f_S(\delta)$, with the concomitant increase in magnitude of the carbon diffusion flux, leads to increased nucleation undercooling (ΔT_P), which, in turn, leads to an increased rate of the subsequent peritectic phase transition (δ to γ) due to the higher thermodynamic driving force for the formation of γ below T_P^E. The relationship between ΔT_P and the observed high kinetics of the peritectic transition has often been reported by other researchers [14,15], but until now no explanation has been given for the root cause of the existence of ΔT_P.

Fig. 4 shows the effect of the fraction of primary solidified δ on the resulting nucleation undercooling at two different cooling rates. Different values of $\Delta f_S(\delta)$ were obtained by heating to different initial equilibration temperatures (T_i) prior to solidification. A higher initial

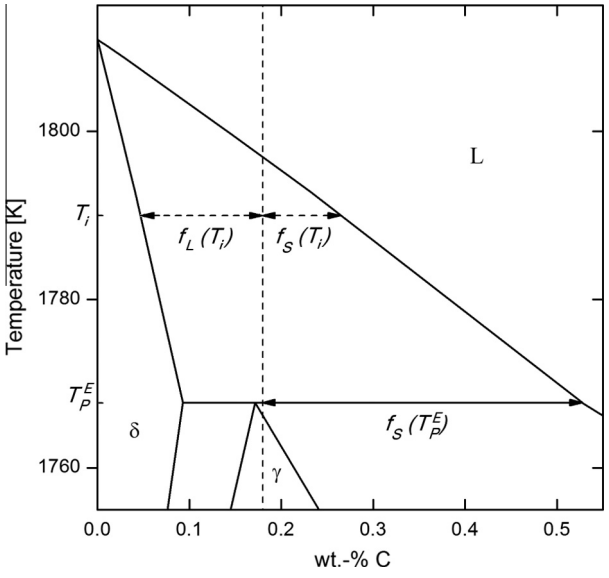

Fig. 2. Schematic illustration of the initial conditions prior to solidification in the Fe–C phase diagram.

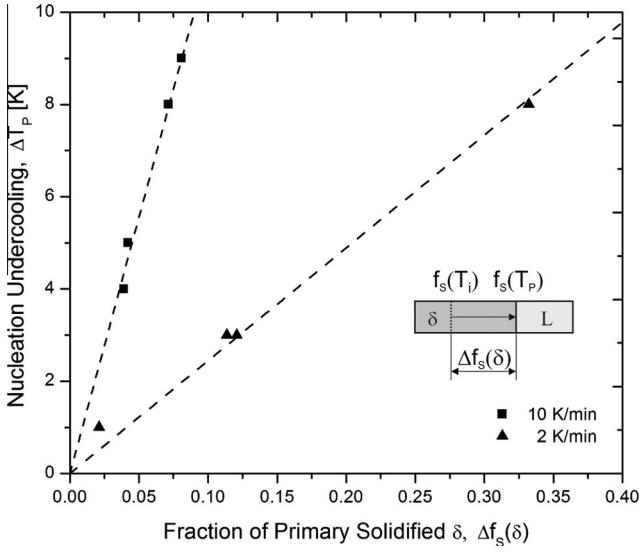

Fig. 4. Influence of the fraction of primary solidified δ on the nucleation undercooling of γ in a Fe–0.18 wt.%C alloy for different cooling rates.

temperature results in a larger initial liquid pool radius and therefore a higher value of $\Delta f_S(\delta)$ prior to γ nucleation, as sketched on the bottom right in Fig. 4. Lower cooling rates lead to shallower solute concentration gradients in δ and allow more time for back-diffusion of the partitioned solute during primary δ solidification. This reduces the diffusional flux during nucleation of the γ phase. Conversely, higher cooling rates result in strong diffusion fields across the L/δ interface, leading to constrained nucleation of γ and higher undercooling (ΔT_P) before nucleation occurs.

4. Discussion

Our experimental observations of solidification occurring close to equilibrium conditions are in agreement with CNT predictions (see Fig. 3) since there are no strong solute diffusion fields present. According to CNT, when the temperature of the L/δ interface drops below the equilibrium peritectic temperature, T_P^E, clusters of γ form at δ grain boundaries that are in contact with the liquid phase due to local fluctuations in concentration, and it is reasonable to suppose that many of the atoms that were in some volume around the precipitate came together to make the nucleus. This would mean that the composition in the matrix is depleted, and how this depletion will influence the growth of the nucleus depends on the time it takes to form a nucleus, compared to how rapidly the species can move around to change the environment in the vicinity of the nucleus [27].

However, upon non-equilibrium solidification and in the presence of solute concentration gradients in the parent phase(s), these clusters form within a solute diffusion field, meaning that from the very beginning these clusters have to allow diffusion fluxes to pass through themselves in a constantly changing environment. In such an environment, the rate of attachment of atoms to the cluster might be different from the rate of atom detachment from the same cluster, depending on the atomic mobility in the adjacent phases. The interaction of atoms surrounding the cluster leads to non-equilibrium thermodynamics, which is not taken into consideration in CNT.

In a thermodynamic open system, the total internal energy U contained in this system is the sum of all forms of energy intrinsic to this system. The total change in internal energy of a system considering internal as well as external influences may be written as:

$$dU = T \cdot dS - P \cdot dV + F \cdot dl + \psi \cdot de + \sum_{i=1}^{n} \mu_i \cdot dN_i + \cdots \tag{1}$$

Eq. (1) relates the total change in internal energy to the sum of the products of intensive variables of temperature T, pressure P, contractile force F, chemical potential μ_i, electrical potential ψ, and the changes in extensive properties of the entropy dS, volume dV, contractile length dl, number of particles dN_i, and electric quantity de [28]. A number of extra terms may be added, depending on the particular system being considered. When the external potential energy of a system, caused by a gravitational, electrical or magnetic field, is held constant during an energy exchange with the environment, the remaining energy change of this system is referred to the change dU of its internal energy U:

$$dU = T \cdot dS - P \cdot dV + \sum_{i=1}^{n} \mu_i \cdot dN_i. \tag{2}$$

The useful or available energy obtainable from such a thermodynamic system for a given temperature and pressure is referred to as the Gibbs free energy, G, which is defined as $G = U + pV - TS$. Substituting Eq. (2) in the total differential of the definition of G yields the change in Gibbs free energy, dG, which determines whether a phase can be thermodynamically stable or not, and can be expressed as follows:

$$dG = V \cdot dP - S.dT + \sum_{i} \mu_i \cdot dN_i. \tag{3}$$

Eq. (3) is one form of the Gibbs fundamental equation [29] where the term containing the chemical potentials accounts for the change in Gibbs free energy results from an influx or outflux of atoms, or in other words, the existence of a surrounding diffusion field. This distinct diffusional flux of solute (in this instance carbon) through the cluster itself interferes with the statistical fluctuations in atom movements that form the cluster and increases the Gibbs free energy barrier to nucleation. It is this increase in Gibbs free energy that leads to an increase in the extent of undercooling required to nucleate the new phase. The clear implication is that the nucleation constraint can be decreased by lowering the diffusion flux or alternatively by decreasing the diffusivity of the solute element(s). In order to test this premise, two experiments were conducted. In the first experiment the flux of carbon in a Fe–C alloy was deliberately changed so as to induce nucleation, as discussed below and shown in Fig. 5, while in the second experiment the extent of undercooling achieved in Fe–C alloys was compared to that in Fe–Ni alloys, since the diffusivity of interstitial carbon atoms at the peritectic temperature in Fe–C alloys ($D_C^\delta = 5 \times 10^{-9}\ m^2\ s^{-1}$ [30]) is significantly greater than that of substitutionally dissolved nickel atoms ($D_{Ni}^\delta = 2.1 \times 10^{-11}\ m^2\ s^{-1}$ [15]) in Fe–Ni alloys. Order-of-magnitude calculations have been performed to calculate the extent of the emerging concentration gradients G_i^δ of component i in δ and the resulting solute fluxes J_i^δ across the L/δ interface (i.e. γ nucleation site) using diffusion modelling software [31–33]. These calculations could be done with confidence since our earlier work has clearly shown that it is justified to use these simulations to estimate diffusion fluxes in our concentric solidification experiments [24,25]. Experimental determination of the emerging concentration gradients was not possible, since in the Fe–C alloys the very high diffusivity

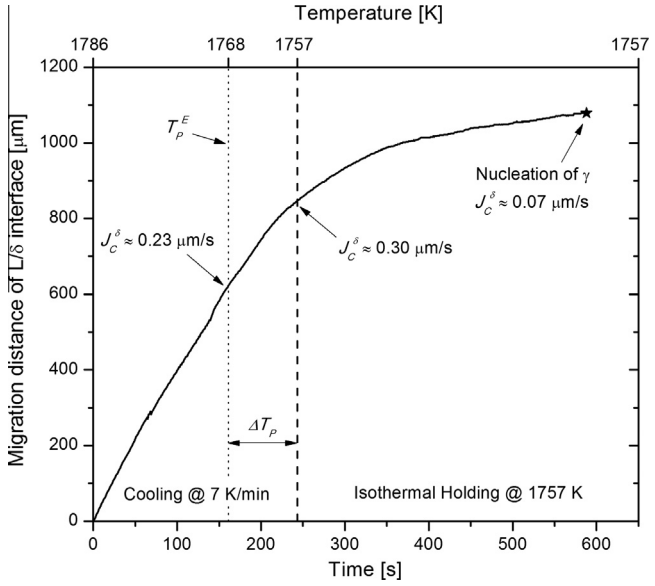

Fig. 5. Progression of the L/δ interface and emerging carbon diffusion fluxes J_C^δ during primary solidification of δ with an effective cooling rate of 7 K/min and subsequent isothermal holding at 1757 K ($\Delta T_P = 11$ K) in a Fe–0.10 wt.%C alloy.

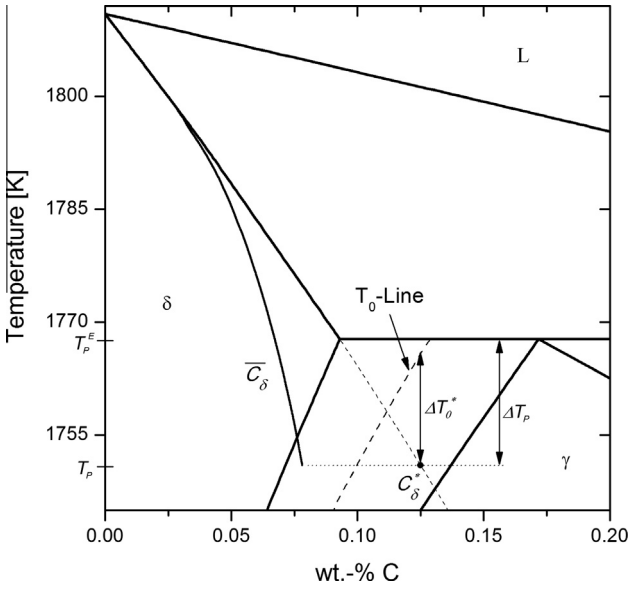

Fig. 7. Section of the Fe–C phase diagram showing the conditions for a massive transformation of δ to γ for a concentrically solidified Fe–0.10 wt.%C alloy.

of carbon and the subsequent austenite decomposition, masking the higher-temperature transformation, makes it impossible to experimentally determine these concentration gradients at room temperature.

In the first experiment, the progression of the L/δ interface in a Fe–0.10 wt.% C alloy was tracked in situ during primary solidification of δ from an initial temperature $T_i = 1786$ K under an effective cooling rate of 7 K min^{-1}, as shown in Fig. 5. The specimen was then held isothermally at 1757 K, 11 K below the equilibrium peritectic temperature ($\Delta T_P = 11$ K). Nucleation of γ is constrained due to the formation of a concentration gradient of carbon in δ during primary solidification and the resulting diffusion flux of carbon across the L/δ interface. The diffusion flux of carbon was calculated as 0.23 μm s^{-1} at the instant that the equilibrium peritectic temperature is reached (1768 K) and 0.30 μm s^{-1} when cooled to 1757 K. During isothermal holding at 1757 K, back-diffusion of carbon from L to δ leads to a shallower concentration gradient of carbon in the δ-phase with a concomitant decrease in the diffusional flux of carbon through the γ-cluster. This continuous lowering of the diffusional flux decreases the interference with cluster formation (i.e. decreasing the last term in Eq. (3)) and when this flux is low enough, a stable nucleus will form. In this instance a stable γ-nucleus formed after 345 s of elapsed isothermal holding time when the carbon flux was reduced to 0.07 μm s^{-1}.

In the second experiment, specimens of Fe–0.18 wt.% C and Fe–4.2 wt.% Ni alloys, respectively, were concentrically

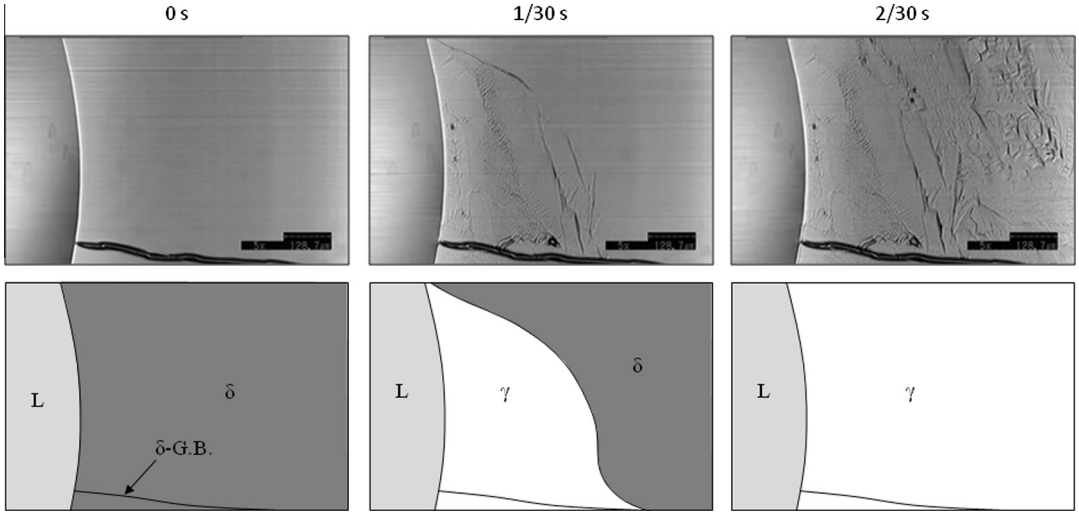

Fig. 6. Massive transformation of δ to γ in a concentrically solidified Fe–0.10 wt.%C alloy at $T_P = 1746$ K ($\Delta T_P = 22$ K) due to diffusional constrained γ nucleation.

solidified under the exact same experimental conditions using a cooling rate of 10 K min^{-1}. In the Fe–0.18 wt.% C alloy, a fraction of primary solidified δ-ferrite, $\Delta f_S(\delta) = 0.07$ resulted in an undercooling of $\Delta T_P \approx 8$ K, whereas in the Fe–4.2 wt.% Ni alloy a much higher fraction of primary solidified δ-ferrite, $\Delta f_S(\delta) = 0.34$ resulted in much lower undercooling, $\Delta T_P \approx 1$ K. The solute concentration gradients in δ prior to γ nucleation were in the range of $G_C^{\delta} \approx 30$ m^{-1} and $G_{Ni}^{\delta} \approx 350$ m^{-1}, respectively. Even though the concentration gradient of nickel was approximately ten times higher than that of carbon, the higher diffusivity of carbon led to a much higher flux $J_C^{\delta} \approx 0.15$ μm s^{-1} of carbon atoms compared to the flux $J_{Ni}^{\delta} \approx 0.007$ μm s^{-1} of nickel atoms. The finding that the significantly smaller nucleation undercooling in the Fe–Ni alloy is due to the lower diffusion fluxes of substitutionally dissolved nickel atoms compared to the strong fluxes of interstitial carbon atoms in the Fe–C alloy provides convincing experimental evidence of the premise that constrained nucleation of γ results neither from the amount of primary phase present, nor from the pertaining concentration gradient, but is the result of the diffusional solute flux J_i through the γ nuclei (see Fig. 1), thus increasing the Gibbs free energy barrier to nucleation.

A frequent observation that is linked to high nucleation undercoolings in peritectic systems is the occurrence of massive transformations. Fig. 6 shows the observed progress of a massive transformation of δ to γ in a concentrically solidified Fe–0.10 wt.% C alloy. According to the principles of thermodynamics, massive transformation can occur if the free energy of the system is reduced by transforming one phase directly into another. The thermodynamic condition for a massive transformation to occur is that the Gibbs energy of the product phase is smaller than that of the parent phase for the same composition. The critical limit for such a transformation is the allotropic phase boundary, which is often denoted by T_0, which is the condition where two phases have the same Gibbs free energy value if they had the same composition.

When nucleation of the γ-phase in Fe–C alloys is sufficiently constrained via diffusive suppression, so that the temperature of the L/δ interface drops below the T_0 temperature of the corresponding composition (allotropic phase boundary), C_{δ}^{*} in Fig. 7, massive transformation of δ to γ can occur. Such a massive-type of transformation has frequently been observed in peritectic systems [14,15,18–20,24], but the underpinning reason for the occurrence of high nucleation undercoolings causing such a transformation has now for the first time been clarified.

5. Conclusion

We have presented for the first time an in situ quantification of the dependency of the early nucleation process on the presence of solute diffusion fields in the direct vicinity of the newly forming cluster. We showed using thermodynamic and kinetic arguments that the Gibbs free energy barrier for nucleation of an intermediate phase is strongly influenced by the atomic mobility and thus must not be neglected in modern nucleation theory. We conclude that the current models do not accurately predict the phase transformation kinetics during peritectic solidification, and that future nucleation models should take into account the atomic mobility and kinetics of the diffusion process around the cluster as well. This is of special importance for systems with high atomic mobility such as high-temperature phase transformations, but might be negligible for phase transformations at lower temperatures. Furthermore, we have identified the root cause for the massive type of transformation in steels that undergo a peritectic phase transition during casting. From a technological perspective, these new insights are of great importance to advanced materials production processes, which relies heavily on nucleation and growth models to design and produce tailor-made materials.

Acknowledgments

Financial support by the Austrian Federal Government (in particular from the Bundesministerium für Verkehr, Innovation und Technologie and the Bundesministerium für Wirtschaft und Arbeit) and the Styrian Provincial Government, represented by Österreichische Forschungsförderungsgesellschaft mbH and by Steirische Wirtschaftsförderungsgesellschaft mbH, within the research activities of the K2 Competence Centre on “Integrated Research in Materials, Processing and Product Engineering”, operated by the Materials Center Leoben Forschung GmbH in the framework of the Austrian COMET Competence Centre Programme, is gratefully acknowledged. We also acknowledge the financial support and availability of the experimental facilities from the University of Wollongong.

References

[1] Myerson AS, Trout BL. Science 2013;341:855.
[2] Yoreo JD. Nat Mater 2013;12:284.
[3] Offerman SE, van Dijk NH, Sietsma J, Grigull S, Lauridsen EM, Margulies L, et al. Science 2002;298:1003.
[4] Kerr HW, Kurz W. Int Mater Rev 1996;41:129.
[5] Goldman AI, Kong T, Kreyssig A, Jesche A, Ramazanoglu M, Dennis KW, et al. Nat Mater 2013;12:714.
[6] Rasche B, Isaeva A, Ruck M, Borisenko S, Zabolotnyy V, Buechner B, et al. Nat Mater 2013;12:422.
[7] Babu NH, Shi Y, Iida K, Cardwell DA. Nat Mater 2005;4:476.
[8] Cloots R, Koutzarova T, Mathieu JP, Ausloos M. Supercond Sci Technol 2005;18:R9.
[9] Cisse J, Kerr HW, Bolling GF. Metall Trans 1974;5:633.
[10] Arnberg L, Baeckerud L, Klang H. Met Technol 1982;9:1.
[11] Arnberg L, Baeckerud L, Klang H. Met Technol 1982;9:7.
[12] Suarez OM, Perepezko JH. In: Cutshall ER, editor. Light metals 1992. TMS; 1992. p. 851.
[13] Xia G, Bernhard C, Ilie S, Fürst C. Steel Res Int 2011;82:230.
[14] Shibata H, Arai Y, Suzuki M, Emi T. Metall Mater Trans B 2000;31:981.
[15] Arai Y, Emi T, Fredriksson H, Shibata H. Metall Mater Trans A 2005;36:3065.

[16] Dippenaar R, Bernhard C, Schider S, Wieser G. Metall. Mater Trans B 2013. http://dx.doi.org/10.1007/s11663-013-9844-6.
[17] Jacot A, Sumida M, Kurz W. Acta Mater 2011;59:1716.
[18] Yasuda H, Nagira T, Yoshiya M, Sugiyama A, Nakatsuka N, Kiire M, et al. IOP Conf Ser: Mater Sci Eng 2012;33. http://dx.doi.org/10.1088/1757-899X/33/1/012036.
[19] Yasuda H, Nagira T, Yoshiya M, Uesugi M, Nakatsuka N, Kiire M, et al. IOP Conf Ser: Mater Sci Eng 2011;27:012084.
[20] Dhindaw BK, Antonsson T, Tinoco J, Fredriksson H. Metall Mater Trans A 2004;35:2869.
[21] Christian JW. The theory of transformations in metals and alloys. Oxford, United Kingdom: Pergamon; 1981.
[22] Reid M, Phelan D, Dippenaar R. ISIJ Int 2004;44:565.
[23] Griesser S, Dippenaar R. CSSCR2013. Stockholm, Sweden and Helsinki, Finland; 2013.
[24] Griesser S. PhD thesis, University of Wollongong; 2013.
[25] Griesser S, Reid M, Pierer R, Bernhard C, Dippenaar R. ICS2012. Germany: Dresden; 2012.
[26] Griesser S, Pierer R, Reid M, Dippenaar R. J Microsc 2012;248:42.
[27] Jackson KA. Kinetic processes. Weinheim: Wiley-VCH; 2004.
[28] Demirel Y. Nonequilibrium thermodynamics. Amsterdam: Elsevier; 2007.
[29] Müller I. A history of thermodynamics—the doctrine of energy and entropy. Berlin: Springer Verlag; 2007.
[30] Ueshima Y, Mizoguchi S, Matsumiya T, Kajioka H. Metall Mater Trans B 1986;17:845.
[31] Andersson JO, Helander T, Höglund L, Shi PF, Sundman B. Calphad 2002;26:273.
[32] Thermo-Calc Software, TCFe6 steels/felloys database version 6. <www.thermocalc.com>.
[33] Thermo-Calc Software. MOB2 alloys mobility database. <http://www.thermocalc.com>.